NASA/TM—2013-217824

Shock Position Control for Mode Transition in a Turbine Based Combined Cycle Engine Inlet Model

Jeffrey T. Csank and Thomas J. Stueber
Glenn Research Center, Cleveland, Ohio

January 2013

NASA STI Program . . . in Profile

Since its founding, NASA has been dedicated to the advancement of aeronautics and space science. The NASA Scientific and Technical Information (STI) program plays a key part in helping NASA maintain this important role.

The NASA STI Program operates under the auspices of the Agency Chief Information Officer. It collects, organizes, provides for archiving, and disseminates NASA's STI. The NASA STI program provides access to the NASA Aeronautics and Space Database and its public interface, the NASA Technical Reports Server, thus providing one of the largest collections of aeronautical and space science STI in the world. Results are published in both non-NASA channels and by NASA in the NASA STI Report Series, which includes the following report types:

- TECHNICAL PUBLICATION. Reports of completed research or a major significant phase of research that present the results of NASA programs and include extensive data or theoretical analysis. Includes compilations of significant scientific and technical data and information deemed to be of continuing reference value. NASA counterpart of peer-reviewed formal professional papers but has less stringent limitations on manuscript length and extent of graphic presentations.

- TECHNICAL MEMORANDUM. Scientific and technical findings that are preliminary or of specialized interest, e.g., quick release reports, working papers, and bibliographies that contain minimal annotation. Does not contain extensive analysis.

- CONTRACTOR REPORT. Scientific and technical findings by NASA-sponsored contractors and grantees.

- CONFERENCE PUBLICATION. Collected papers from scientific and technical conferences, symposia, seminars, or other meetings sponsored or cosponsored by NASA.

- SPECIAL PUBLICATION. Scientific, technical, or historical information from NASA programs, projects, and missions, often concerned with subjects having substantial public interest.

- TECHNICAL TRANSLATION. English-language translations of foreign scientific and technical material pertinent to NASA's mission.

Specialized services also include creating custom thesauri, building customized databases, organizing and publishing research results.

For more information about the NASA STI program, see the following:

- Access the NASA STI program home page at *http://www.sti.nasa.gov*

- E-mail your question to *help@sti.nasa.gov*

- Fax your question to the NASA STI Information Desk at 443–757–5803

- Phone the NASA STI Information Desk at 443–757–5802

- Write to:
  STI Information Desk
  NASA Center for AeroSpace Information
  7115 Standard Drive
  Hanover, MD 21076–1320

NASA/TM—2013-217824

Shock Position Control for Mode Transition in a Turbine Based Combined Cycle Engine Inlet Model

Jeffrey T. Csank and Thomas J. Stueber
Glenn Research Center, Cleveland, Ohio

Prepared for the
45th Combustion/33rd Airbreathing Propulsion/33rd Exhaust Plume and Signatures/27th Propulsion Hazards Joint Subcommittee Meeting
sponsored by the Joint Army-Navy-NASA-Air Force (JANNAF)
Monterey, California, December 3–7, 2012

National Aeronautics and
Space Administration

Glenn Research Center
Cleveland, Ohio 44135

January 2013

Acknowledgments

The authors would like to thank the Fundamental Aeronautics Program's Hypersonics project for funding this work.

This work was sponsored by the Fundamental Aeronautics Program at the NASA Glenn Research Center.

Level of Review: This material has been technically reviewed by technical management.

Available from

NASA Center for Aerospace Information
7115 Standard Drive
Hanover, MD 21076–1320

National Technical Information Service
5301 Shawnee Road
Alexandria, VA 22312

Available electronically at http://www.sti.nasa.gov

Shock Position Control for Mode Transition in a Turbine Based Combined Cycle Engine Inlet Model

Jeffrey T. Csank and Thomas J. Stueber
National Aeronautics and Space Administration
Glenn Research Center
Cleveland, Ohio 44135

Abstract

A dual flow-path inlet for a turbine based combined cycle (TBCC) propulsion system is to be tested in order to evaluate methodologies for performing a controlled inlet mode transition. Prior to experimental testing, simulation models are used to test, debug, and validate potential control algorithms which are designed to maintain shock position during inlet disturbances. One simulation package being used for testing is the High Mach Transient Engine Cycle Code simulation, known as HiTECC. This paper discusses the development of a mode transition schedule for the HiTECC simulation that is analogous to the development of inlet performance maps. Inlet performance maps, derived through experimental means, describe the performance and operability of the inlet as the splitter closes, switching power production from the turbine engine to the Dual Mode Scram Jet. With knowledge of the operability and performance tradeoffs, a closed loop system can be designed to optimize the performance of the inlet. This paper demonstrates the design of the closed loop control system and benefit with the implementation of a Proportional-Integral controller, an H-Infinity based controller, and a disturbance observer based controller; all of which avoid inlet unstart during a mode transition with a simulated disturbance that would lead to inlet unstart without closed loop control.

Nomenclature

ADRC	Active Disturbance Rejection Control
AIP	Aerodynamic Interface Plane
CCE	Combined Cycle Engine
CCE-LIMX	Combined Cycle Engine Large Scale Inlet for Mode Transition Experiments
DMSJ	Dual Mode Scramjet
HiTECC	High Mach Transient Engine Cycle Code
HSFP	High Speed Flow Path
LSFP	Low Speed Flow Path
MS	Mixed Synthesis
PI	Proportional–Integral controller
SWT	Supersonic Wind Tunnel
TBCC	Turbine Based Combined Cycle
Pressure recovery	Diffuser total exit pressure divided by free stream atmospheric pressure
Pressure ratio	Diffuser static pressure divided by free-stream pressure atmospheric pressure
Mass flow ratio	Mass-flow rate through the inlet divided by inlet capture mass-flow rate

Introduction

The National Aeronautics and Space Administration (NASA) is exploring the use of reliable airbreathing launch vehicles for hypersonic flight through Earth's atmosphere and to provide routine airline-type access to space. To accomplish these objectives, the Fundamental Aeronautics Program's Hypersonics project is investigating a Turbine Based Combined Cycle (TBCC) propulsion system, consisting of a turbine and a dual-mode scramjet (DMSJ) combustor, for horizontal take-off and acceleration to hypersonic speeds.

The TBCC propulsion system features a split-flow inlet that is capable of directing airflow to either or both of the engines—a turbine engine and a DMSJ combustor. The technical challenge being addressed in this research is the transitioning of airflow from the turbine engine to the DMSJ with minimal loss of net thrust. This activity is referred to as inlet mode transition. A concern is that during this transition, the inlet may unstart due to a rapid change in the subsonic diffuser static pressure. The static pressure change can be due to noise in the system from unsteady flow or a system disturbance. The challenge is to maintain sufficient operability and performance of the propulsion system throughout the inlet mode transition event. Operability is defined as the margin of diffuser static pressure that does not result in an inlet unstart, also known as the stability margin, while performance is defined as a pressure recovery goal and tolerance of flow distortion. These objectives led the NASA Hypersonic team to design, develop, and fabricate an inlet system suitable for experimental testing in the GRC 10- by 10-ft supersonic wind tunnel (SWT) to study inlet mode transition.

The experimental system is an integrated dual flowpath inlet known as the Combined Cycle Engine Large-scale Inlet for Mode transition eXperiments (CCE-LIMX) (Ref. 1). The design is such that one flow path can direct airflow to a turbine and the other can direct airflow to a DMSJ. The work addressed in this paper considers the dynamic operability and performance of the flow path designed to serve the turbine engine.

Experiments in the SWT are segmented into three phases. To date, the testing for Phase 1 and 2 has been completed and the analysis work is ongoing. The first phase studied the CCE-LIMX operability and performance at steady-state conditions. One of the Phase 1 products was a steady-state inlet mode transition schedule that discretely identified inlet operating conditions that must be passed through while performing an inlet mode transition. Characteristics of acceptable operating points are those with maximum performance, specifically pressure recovery, while maintaining operability with clean airflow–low flow distortion to the engine. When defining the operating points, objectives which maximize inlet performance are sacrificed to reach an acceptable stability margin while avoiding excessive distortion. The second phase of testing was to perform system identification experiments at the defined inlet mode transition operating points. Data from the Phase 2 experiments are reduced to control design models to support controls research at each operating point. The controls research is to design a closed loop control algorithm that can reject inlet disturbances and afford the opportunity to operate the inlet at more aggressive conditions or with a reduced stability margin. The third phase will be to test candidate control algorithms.

The illustration in Figure 1 is a computer aided design replication of the CCE-LIMX as mounted in the Glenn Research Center’s supersonic wind tunnel—airflow is from left to right. The CCE-LIMX has an over-mounted low speed flow path (LSFP) and an under-mounted high speed flow path (HSFP). During inlet mode transition, the splitter will rotate clockwise towards LSFP close-off. The variable ramp can be raised, or lowered, to change the cross sectional area of the LSFP throat. The desired throat area is scheduled based upon free stream conditions. At the aft end of the LSFP subsonic diffuser, the aerodynamic interface plane (AIP) is where the turbine engine is normally mounted; however, the CCE-LIMX configuration has a cold pipe and mass-flow plug system in lieu of the turbine engine. Also at the aft end of the diffuser are overboard bypass doors that can be opened to vent and reduce the air pressure in the diffuser. The diagram of the CCE-LIMX inlet shown in Figure 1 is configured for supersonic operation, vehicle speed of Mach 4.0, prior to and during mode transition. For this state, most of the captured air is directed through the LSFP to the turbine engine.

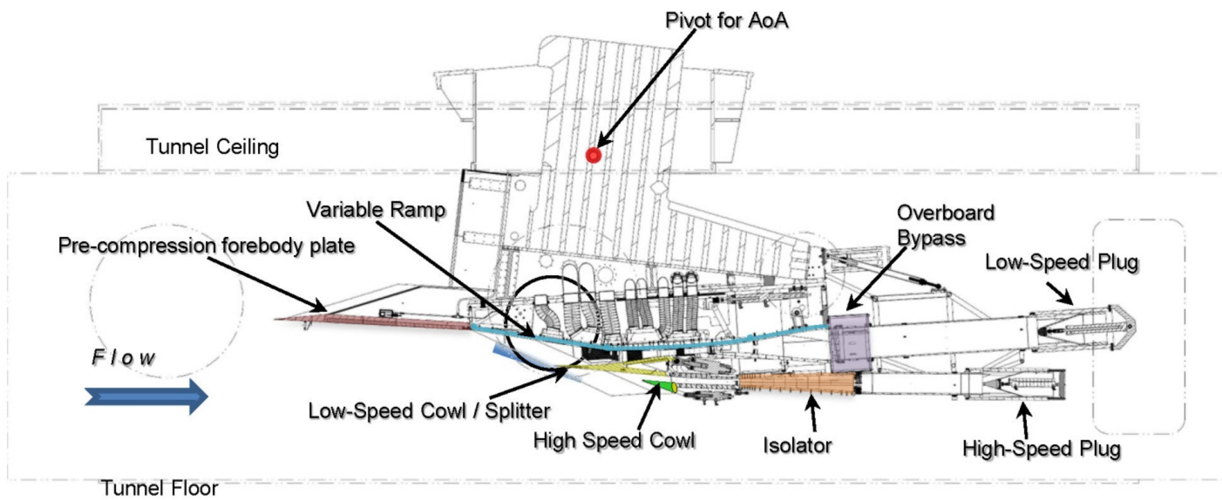

Figure 1.—Diagram of the CCE-LIMX inlet shown in its designed Mach 4.0 configuration.

The main function of the LSFP is to convert the kinetic energy of the incoming air into a static pressure rise and provide a uniform flow at the AIP. In general, the ratio of total pressure measured at the AIP relative to free stream, known as the pressure recovery, increases and flow distortion decreases as the terminal shock moves upstream towards the throat, making it desirable to operate the shock as close as possible to the throat. An airflow disturbance upstream of the inlet due to an atmospheric pressure drop or a downstream pressure rise from the turbine engine may cause the normal shock to move upstream from the throat and be expelled from the flow path. This is known as inlet unstart.

The use of bypass doors as an actuator to regulate pressure ratio, the ratio of diffuser static pressure relative to free stream, has been successful for keeping supersonic inlets started (Refs. 2, 3,and 4). For an axisymmetric, mixed compression inlet designed for Mach 2.5, a control system was implemented using a 110 Hz bypass door system and 250 Hz diffuser pressure measurement as the feedback variable. The control system was shown to reduce the normal shock movement due to a disturbance up to a frequency of 40 Hz, just below the inlet's resonant frequency of 55 Hz.

In parallel to the first two phases of wind tunnel testing, NASA is designing controllers based on computational simulations with the High Mach Transient Engine Cycle Code (HiTECC); which is the topic of this paper. HiTECC (Ref. 5) is a combined cycle engine (CCE) simulation tool featuring a turbine engine and a DMSJ propulsion system model, nozzle models, a heat transfer model, fuel flow models, hydraulics models, etc. The HiTECC tools consist of the following four building blocks, a propulsion system(Ref. 6), a thermal management and fuel system model (Ref. 7), hydraulics and kinematics model (Ref. 8), and finally a control system. The HiTECC inlet model and propulsion system has been modified to be representative of the CCE-LIMX (Ref. 9). The modifications included replacing the propulsion system engine models with a cold pipe and mass-flow plug system, as done with the experimental system and adding a simulated bypass door at the aft end of the diffuser. The bypass door is opened and closed via a 2.36 in. linear actuator with a maximum exit area of 3.57 in.^{2}. The bypass door is capable of operating up to 77 Hz and is modeled as an under damped unity gain transfer function with a damping factor of 0.6266 and includes saturation limits. The actuator model does not include rate limits. This configuration, referred to as the HiTECC wind tunnel model, is used in this paper for proposing, designing, testing, and evaluating potential control algorithms before implementation on the CCE-LIMX.

This paper focuses on the design process for a closed loop controller to ensure operability of the inlet during mode transition even in the presence of an external disturbance using the HiTECC simulation. The next section of this paper will discuss the development of a mode transition schedule and simulation of a mode transition without active feedback control. Linear models of the diffuser will be discussed followed by the closed loop controller design and results.

Mode Transition

As part of the CCE-LIMX Phase 1 experiments, data is collected to plot the total pressure recovery with respect to the engine flow ratio. These plots are called total pressure characteristic curves or the “cane” curve due to its shape like a cane. This map is created by plotting the steady-state pressure ratio measurements (diffuser exit pressure divided by free stream atmospheric pressure) against the mass-flow ratio (mass-flow rate through the inlet divided by inlet capture mass-flow rate) for varying splitter angles and LSFP mass-flow plug positions. This is standard practice for characterizing supersonic inlets in a wind tunnel using a cold-pipe and mass flow plug in lieu of a turbine, because the data to report total pressure recovery requires pressure sensor rakes at the AIP (Ref. 10). A rake of sensors at the AIP is not expected to be available when a turbine is installed. Since a control system is intended to be useful for tests with or without the turbine, this work assumes the pressure rakes at the AIP are not available. The control system is designed using the diffuser static pressure; therefore, instead of plotting the pressure recovery, the pressure ratio (ratio of diffuser static pressure measurements to free-stream) will be plotted against the mass-flow ratio. The relationship between the diffuser pressure ratio and mass-flow ratio at a splitter angle results in a cane shaped curve as shown in Figure 2.

The curve in Figure 2 contains the following three segments: a vertical section, a horizontal section, and a transition region also referred to as the “knee”. The vertical section of the cane-curve occurs when the normal shock is located aft of the stability bleed region. This placement of the shock occurs when the diffuser static pressure is low. Because inlets operating in this region will have supersonic flow over the bleeds, slightly perturbing the position of the mass-flow plug, or bypass door, will change the pressure ratio but will have little to no change in the mass-flow ratio. Inlets operating at the top end of this region have the desired high performance. Operating points on the lower part of the vertical segment of the cane curve typically have higher distortion measurements that may exceed turbine engine tolerance.

The knee of the cane-curve occurs when the normal shock is close to or partially covers the passive stability bleeds. The knee forms because mass flow losses will increase as the shock progresses upstream into the bleed region. Small perturbations in the diffuser pressure ratio will results in a change in mass flow ratio. An inlet operating in this region can be moved back to the vertical region by opening the

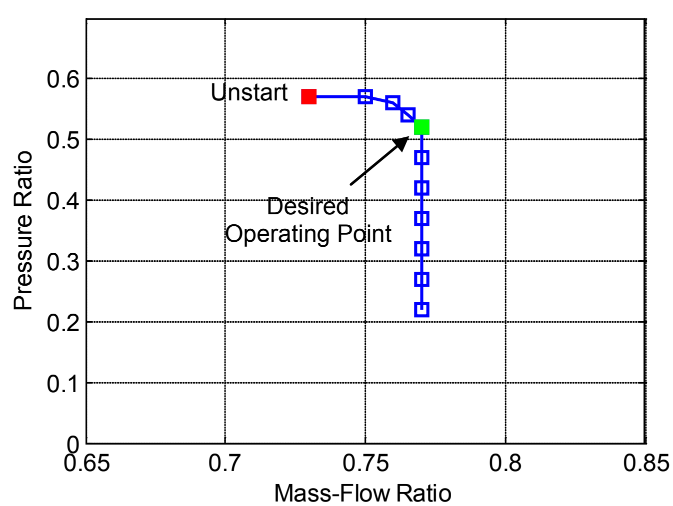

Figure 2.—Example cane-curve. The red box is the last steady-state point recorded before the inlet unstarts and the green box is the desired operating point.

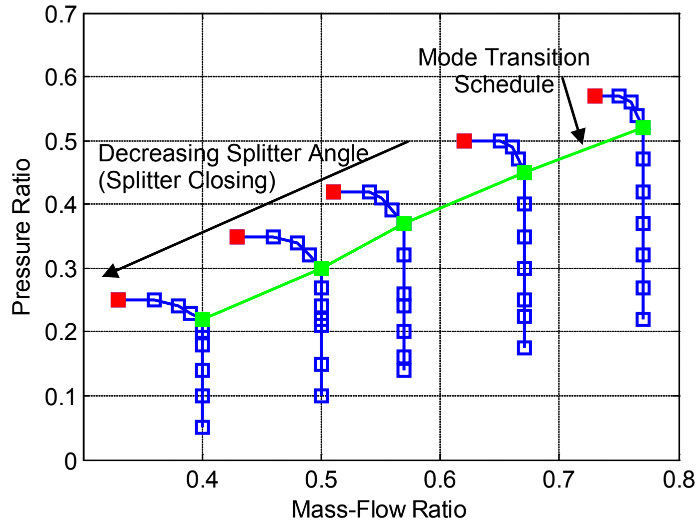

Figure 3.—Example mode transition curve created by plotting cane-curves at several splitter locations.

bypass doors to decrease the pressure ratio. Multiple cane-curves can be created and plotted on the same chart at various discrete splitter positions. Finally, the selected operating points of each cane curve can be connected to create a mode transition schedule as the splitter rotates towards LSFP close-off as shown in Figure 3. Mode transition is continuous, but the schedule is created from limited test data at specific splitter angles.

The HiTECC simulation does not contain detailed computational fluid dynamics (CFD) code and will not accurately simulate the effect of the normal shock passing over the stability bleeds; therefore, an inlet performance map cannot be created as done in the hardware experimentations. To create a mode transition schedule using HiTECC, an alternative method is employed where the mass-flow plug is inserted towards cold pipe close-off and the steady-state diffuser static pressure ratio and shock locations are recorded at varying splitter angles as shown in Figure 4. The shock locations, indicated by the abscissa on the Figure 4 chart, are measurements from the bow tip of the vehicle. Therefore, as shock location increases the shock is located further downstream; whereas, a shock that moves upstream will have decreasing shock location values. The inlet will unstart if the shock location moves upstream of the 162 in. mark. For this process, the mode transition schedule is found by specifying the desired normal shock location. The empirical approach does not have a shock location sensor and therefore uses the cane curves to estimate the shock location; whereas, the HiTECC approach actually calculates the shock location as part of its process. Figure 4 shows the mode transition schedule for a desired shock location of 167 in. This method reveals desired pressure ratios for maintaining the normal shock at specific locations for various splitter positions. Even though there are small differences in the mechanics, the resulting mode transition schedule is a collection of desired pressure ratios as a function of the splitter angle.

During mode transition the turbine engine power level is decreased. This in turn decreases the turbine mass flow which will increase the LSFP diffuser static pressure. The event can be simulated with the CCE-LIMX by further inserting the mass-flow plug toward cold-pipe close-off. Increasing the diffuser pressure at the LSFP AIP will also move the normal shock upstream and decrease the operability of the inlet—more susceptible to unstart. Furthermore, closing off the splitter will also decrease the captured mass flow and the static pressure upstream of the normal shock, also allowing the normal shock to move towards the front of the inlet. An open loop controller can be designed using a bypass door located in the diffuser which is opened as a function of splitter angle and decrease the back pressure at the LSFP AIP. This results in a HiTECC based open loop control method.

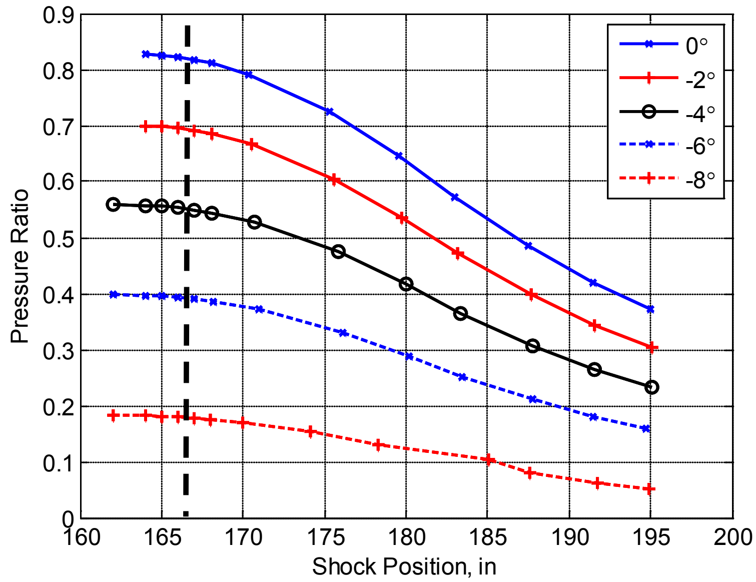

Figure 4.—Diffuser pressure ratio versus shock position location at various splitter angles (degrees).

For the mode transition simulations, the splitter will be closed from an angle of 0 to -7.5° between 0.5 and 2.0 s and the mass flow plug moves an additional 0.25 in. linearly towards cold-pipe close-off. Beyond a splitter angle of -7.5°, the bypass doors are fully opened to maintain supersonic airflow through the throat. The simulation results using the open loop control method are shown in Figure 5 with the pressure ratio (middle plot) and shock location (bottom plot) graphed with respect to time. In the bottom plot of Figure 5, the location of the throat where inlet unstart will occur is identified with a black dotted line. Figure 5 indicates that the inlet remained started during the mode transition.

A disturbance is added to the system (shown in Figure 6) to determine if the inlet will remain started while performing a mode transition. The disturbance input magnitude for the design process was chosen to be approximately the same size as the control actuator, bypass door, with a frequency of 20 Hz. The disturbance is added to the system by modifying the exit area of the diffuser, or adding an additional disturbance door as will be done in the wind tunnel experiments. Decreasing the disturbance increases the pressure while increasing the disturbance input decreases the pressure. At the beginning of the simulation, the disturbance increases the exit area by 3.49 in.^{2} and the mass flow plug is positioned to provide the desired pressure ratio. At a time of 0.7 s into the simulation, the disturbance is decreased to zero, increased at a time of 1.25 s, and decreased to zero again at 2.3 s. Only the first 0.8 s of the simulation with the disturbance added to the mode transition is illustrated in Figure 7 because the inlet unstarts shortly after the initial step disturbance input. The drop in shock location below the unstart dotted line illustrated in the lower chart in Figure 7 shows that the inlet does indeed unstart when the disturbance is initially decreased at a time of 0.7 s. Simply scheduling the bypass door input during mode transition in an open-loop fashion is unable to decrease the back pressure in response to the disturbance and unstart occurs. To mitigate the effect of the disturbance on shock position, closed loop control solutions will be studied.

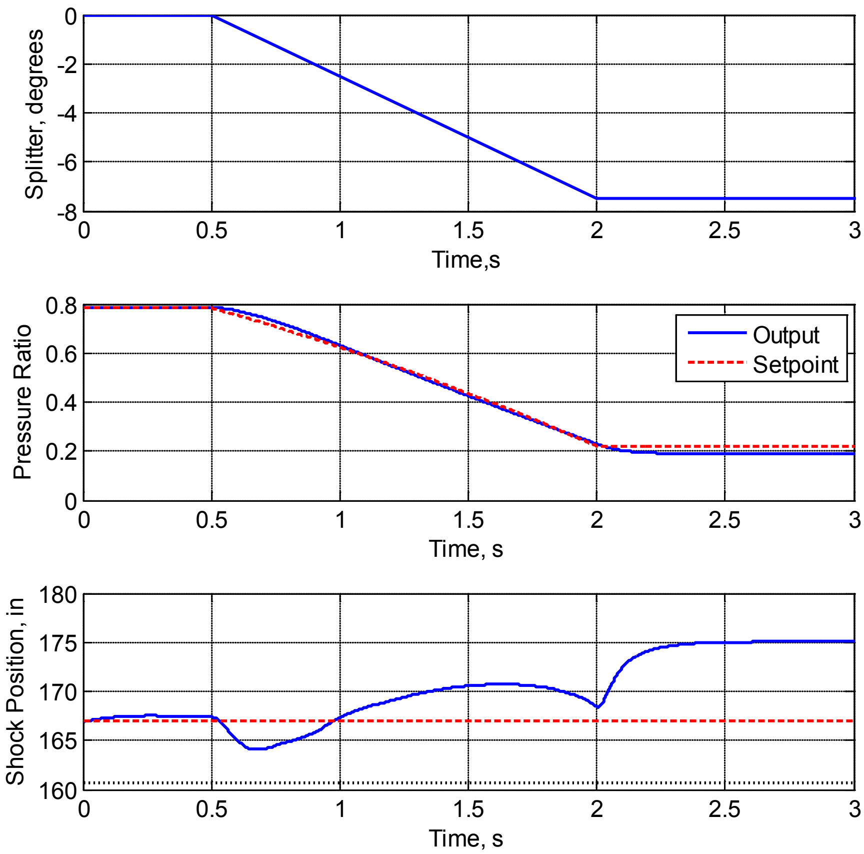

Figure 5.—Open loop results showing the splitter angle command (top), the diffuser pressure ratio (middle) and shock location (bottom).

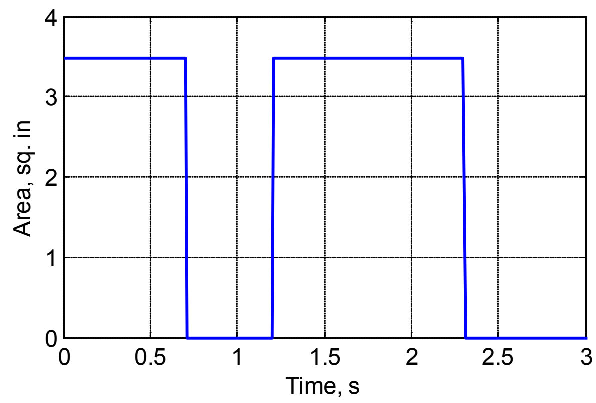

Figure 6.—Disturbance input profile.

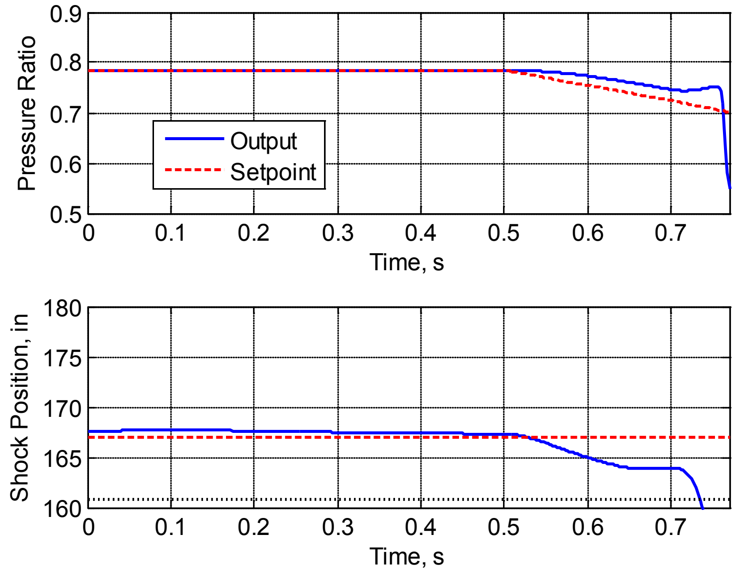

Figure 7.—Open loop mode transition results showing the diffuser pressure ratio (top) and shock location (bottom) with the disturbance input added.

Linear Model

Linear models are developed to aid in the control design process. The linear models will be developed empirically using the HiTECC tool. This approach applies a sine-sweep perturbation pattern, starting from a frequency of 0.01 to 50 Hz. This signal is applied to the bypass door exit area of the diffuser and includes the unity gain dynamics of the bypass door actuator. In addition, a step change command will be applied with the same magnitude of the sine sweep. Using sine sweep results, linear models can be obtained using the MATLAB (The MathWorks, Inc.) *arx* command (provided in the MATLAB System Identification Toolbox). The step response of the linear model is then compared to the recorded step response test from the HiTECC simulation using the MATLAB *compare* function to determine the accuracy of the linear model. The resultant linear system is a single input single output system (SISO) process, with the input being the open exit area in the diffuser and output being the diffuser pressure ratio, with the bypass gate dynamics included. Using the *arx* command, the linear model (exit area to pressure ratio) at Mach 3.75 flight condition, with a steady-state initial shock location of 173 in., is described with the following continuous time transfer function:

$$tf(s) = \frac{-13.4929(s+768.6)(s^2+1238s+778600)}{(s+13.02)(s+234.1)(s^2+77.83s+72080)} \tag{1}$$

This linear model is only valid at the Mach 3.75 flight condition, with the splitter fully open, and a steady state shock location of 173 in. A Bode plot comparison of the linear models at the Mach 3.75 flight condition and at various steady state shock locations are shown in Figure 8. As the linearization point moves downstream, the subsonic volume decreases. This is represented in the linear model as a loss in system gain and can be seen in Figure 8 by the decrease in gain near steady-state as the shock moves further downstream. In addition to this change, the natural frequency increases as the shock moves downstream. Bode plots can also be developed at a consistent shock location, 173 in., and with a varying splitter angle as shown in Figure 9. This Bode plot shows that the system losses gain as the splitter rotates towards LSFP close-off and the natural frequency of the resonant poles increase. Since the dynamics of the diffuser inside the desired control bandwidth, max 20 Hz, do not greatly change based on the splitter location and steady state shock location, as shown in Figure 8 and Figure 9, the plant model of Equation (1) will be the only model used for control design purposes.

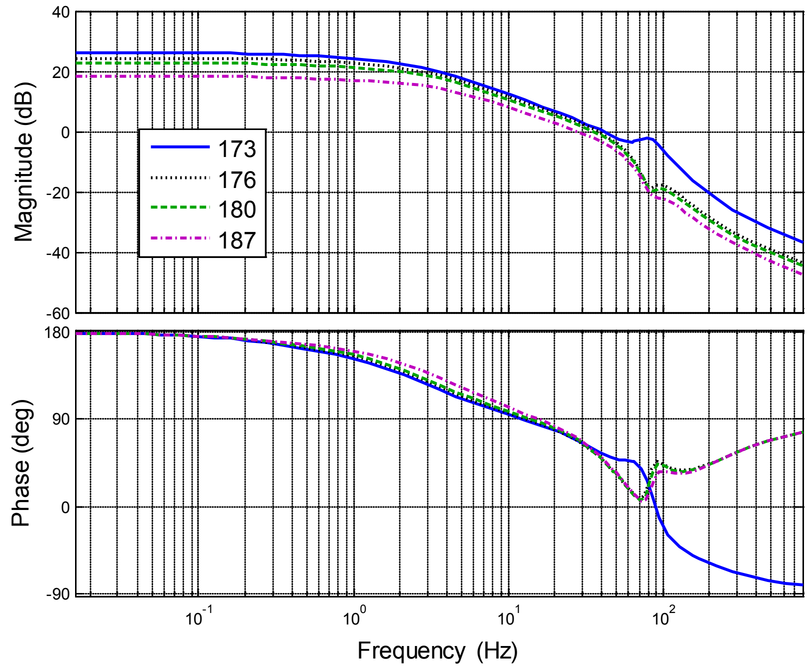

Figure 8.—Bode plot for varying shock location.

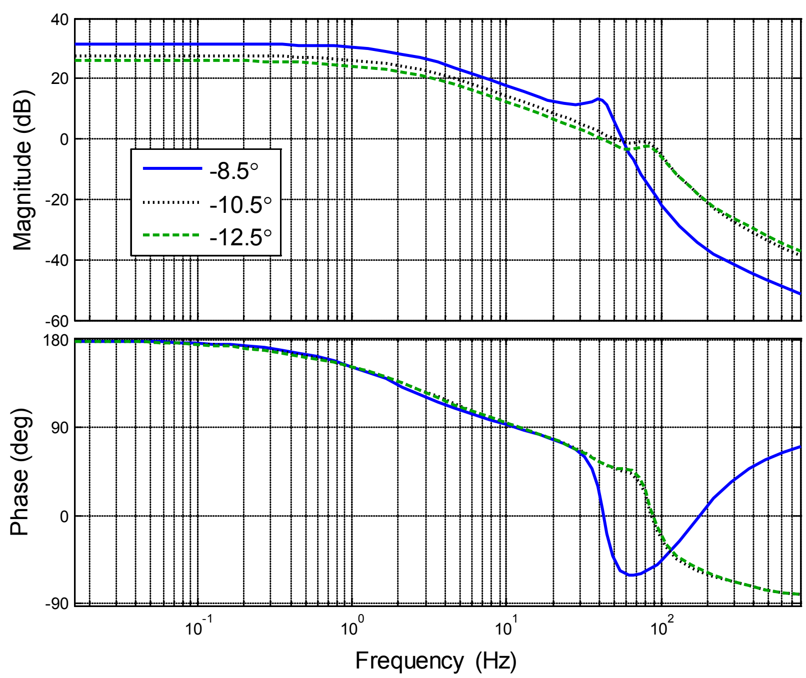

Figure 9.—Bode plot for varying splitter angle.

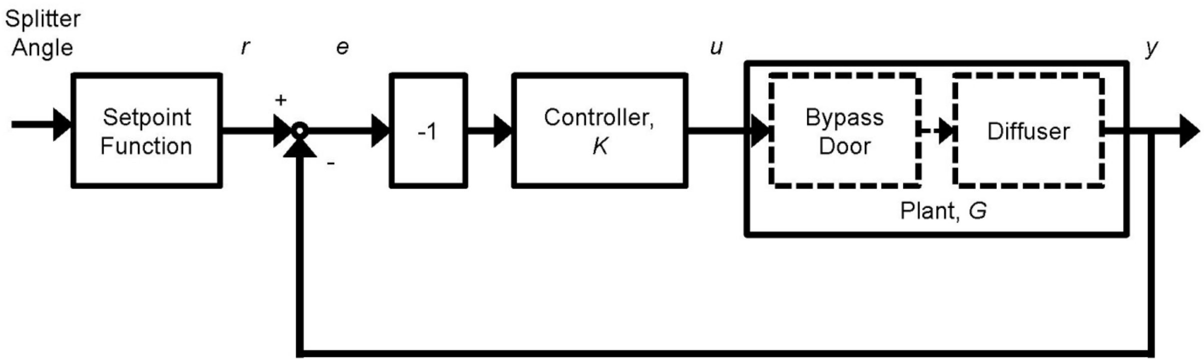

Figure 10.—Closed Loop Control System with an error (e) signal applied to the controller (*K*), which produces a bypass command signal (*u*) applied to the plant (*G*). The measured diffuser static pressure (*y*) is fed back and subtracted from the setpoint (*r*).

Shock Location Control Design

With the relationships between the normal shock location and pressure ratio based on splitter angle defined in Figure 4, a closed loop control system is designed to reject disturbances and increase the operability of the TBCC inlet. The closed loop control system, shown in Figure 10, consists of a setpoint function to calculate the desired pressure ratio, r, based on the splitter angle, a controller, K, and the plant, G, which consists of a bypass door and diffuser which produce the pressure ratio output, y. In this control system the error, e, and the desired control action, u, are inversely related. This means that a decreased command signal results in an increased pressure ratio. Therefore, the error is multiplied by –1. If the feedback is greater than the setpoint, the control command is increased to further open the bypass door to further reduce the pressure ratio.

Proportional-Integral Control

Using the closed loop control system shown in Figure 10, a Proportional-Integral (PI) controller is designed and implemented. The PI control law is:

$$u(t) = -k_p e(t) - k_i \int e(t)dt \quad (2)$$

where $e(t)$ is the error $(r(t) - y(t))$, and k_p and k_i are the PI controller gains. The PI controller gains were set to provide the quickest response time with no overshoot, using trial and error PI tuning methods (Ref. 11). The PI controller was selected to serve as a baseline because it is the most widely used closed-loop controller due to its simplistic control law and ease of tuning. This algorithm does not require extensive knowledge of the process that is being controlled, adding to its popularity.

H-Infinity Mixed Sensitivity Control

The PI controller can be replaced with an optimal controller using the MATLAB *mixsyn* command from the robust toolbox. The *mixsyn* command computes a controller that minimizes the H-Infinity norm for the weighted mixed sensitivity control problem:

$$T_{yu} = \begin{bmatrix} W_1 S \\ W_2 R \\ W_3 T \end{bmatrix} \quad (3)$$

where W_1, W_2, and W_3 are user defined weighting functions, S is the sensitivity function, R is the closed loop transfer function, and T is the complimentary sensitivity function. For tuning, each weight determines the importance of the associated term. General rules for tuning are that the gain of W_1 is usually small inside the desired control bandwidth and is greater outside the control bandwidth to achieve good disturbance attenuation. W_2 defines the shape of the control input, and can be defined as a filter to reduce high frequency spikes from the controller. The weighting function W_3 is typically chosen to be of small magnitude outside the control bandwidth and large inside the control bandwidth to ensure good stability margin.

One method for choosing W_1 is:

$$W_1 = \frac{\left(s/M \right) + w_B}{s + w_B A} \tag{4}$$

where M is the value of W_1 at very high frequencies (infinity), A is the value of W_1 at steady state, and w_B is the desired or approximate bandwidth. These values can be modified to provide the desired performance. Increasing W_B will increase the overall gain of the system and make the response more aggressive. M was chosen to be greater than 1 to ensure that S is smaller at high frequency and A is chosen to be small to amplify S at frequencies less than W_B. Usually W_2 is chosen as a gain, however W_2 can also be a filter to amplify the control signal at low frequencies and filter the control signals at high frequencies.

Active Disturbance Rejection Control

During mode transition, the inlet will be transitioning through operating points that are off the Mach 4 design geometry; therefore, the inlet will be more susceptible to inlet unstart. Pressure disturbances, either negative pressure disturbances from the atmosphere or positive pressure disturbances from the turbine engine will result in increased diffuser pressure ratio, and the normal shock will move upstream. The task to prevent an unstart is to reject the disturbance before the inlet unstarts. To provide better disturbance rejection, a disturbance observer type controller can be implemented. In this paper the active disturbance rejection controller (ADRC) has been chosen due to success in previous disturbance rejection applications (Refs. 12, 13, and 14).

The ADRC controller has three parameters: the DC plant gain (b_0), the controller bandwidth (ω_c), and the observer bandwidth (ω_o). The DC plant gain is found from the transfer function. The controller and observer bandwidths are tuned to provide the best performance, quickest response time with smallest overshoot. Increasing the controller bandwidth makes the control system response more aggressive while increasing the observer bandwidth tends to increase disturbance rejection; however, increasing the observer bandwidth too much can destabilize the system. It has been noted that in most applications, the observer bandwidth is set to 10 times the controller bandwidth (Ref. 14).

Transient Stability Index

A generic approach to analyze and compare the effectiveness of using closed-loop feedback control to maintain stability is to evaluate the system with a transient stability index (TSI) analysis (Ref. 15). For this case, the TSI determines the frequency and percentage of the total airflow that when forced to exit the cold pipe instead of the bypass door causes the inlet to unstart. The TSI evaluation process first determines a stability index (*SI*). The *SI* is determined by opening the bypass door to a specified area and decreasing the cold pipe exit area to obtain a desired steady-state pressure ratio. The stability index is the percentage of airflow through the bypass door with respect to the total airflow captured—captured airflow is the sum of the airflow through the bypass door and past the cold-pipe mass flow plug, or

$$SI = 100\left(\frac{W_{\text{bypass door}}}{W_{cp}}\right) \quad (5)$$

After calculating the *SI*, the bypass door will be closed and reopened at a frequency, *f*. At a given time, t_1, the negative half of a sine wave is applied to the bypass door to close and then reopen the bypass door to the starting area at t_2 determined based on the frequency of the input signal.

An example input curve is shown in Figure 11. If the inlet remains started, the frequency is reduced and the test is once again applied until a frequency is found that results in an inlet unstart. Once the frequency which results in unstart is found, the bypass door area is changed and the SI evaluation process is repeated for the new open area. This process is repeated for multiple bypass door open area settings.

Control Design Results

The proposed control algorithms of the control design section have been implemented in HiTECC. All results are simulated using the same disturbance profile as appeared in the Shock Position Control Design section (Figure 6).

Proportional-Integral Control

A computational simulation of the PI controller proposed has been implemented and tuned. The system response to a PI controlled mode transition with controller gains of k_p = 9.9 and k_i = 21.84 is shown in Figure 12. The PI controller was tuned to maximize the disturbance rejection response time while minimizing overshoot. The top plot of Figure 12 shows the bypass door open area (control effector) for the experiment. Not illustrated is the disturbance door position which is the same as used in the previous simulation. Without closed-loop feedback control, the disturbance input step change would have increased the diffuser pressure ratio to a level that would surely unstart the inlet as shown in Figure 7. The bottom plot in Figure 12 compares the shock location against the setpoint, desired, shock location throughout the experiment. Figure 12 shows that the PI controller successfully rejected the disturbance, thus increasing the operability of the LSFP even though the shock did move forward of the setpoint, but remained downstream from the throat, as the splitter closes.

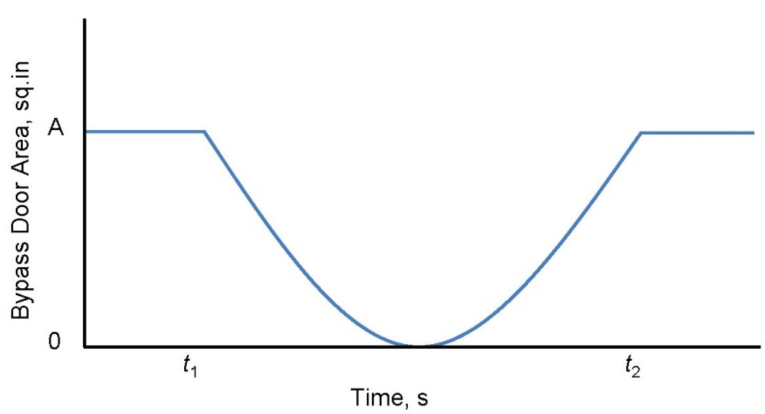

Figure 11.—Bypass door command for creating the transient stability index plot.

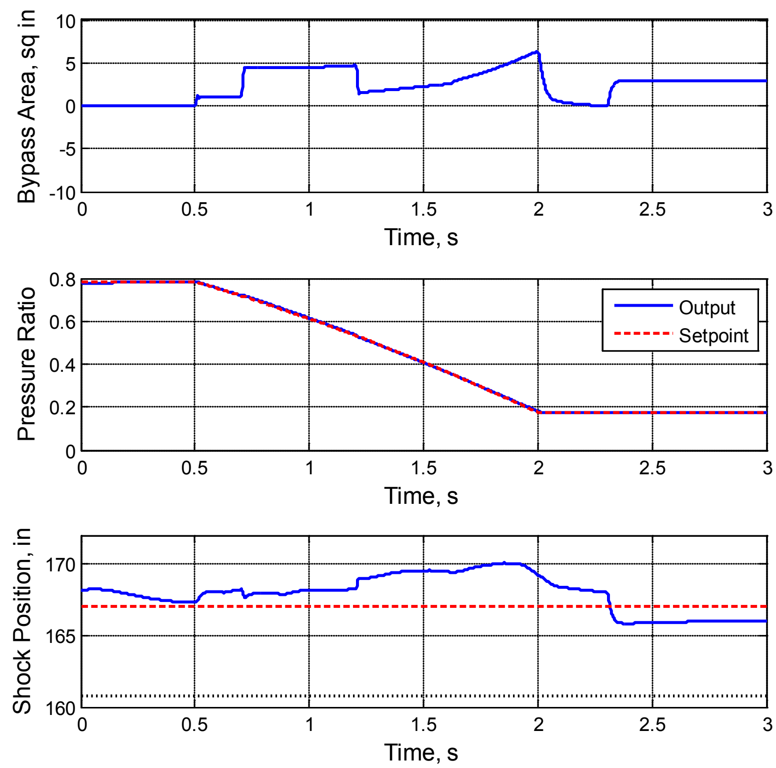

Figure 12.—Control input (top), pressure ratio (middle), and shock position location (bottom) for a PI controlled mode transition with a disturbance step added to the system.

H-Infinity Mixed Sensitivity Control

To design a mixed synthesis controller using MATLAB, the *mixsyn* command requires a plant transfer function, G, with a linear gain from the linear actuator command to actuator door open area, and the user-defined weights from Equation (3). The plant model from Equation (1) is used for the *mixsyn* command. The weighting functions used for finding K are:

$$
\begin{aligned}
W_1(s) &= \frac{\left(s/10\right)+62.8319}{s+0.1948} \\
W_2(s) &= \frac{1}{\left(s/188.4956\right)+1} \\
W_3(s) &= 0
\end{aligned}
\tag{6}
$$

The closed loop simulation with the mixed synthesis controller through mode transition is shown in Figure 13. Again, the same disturbance was applied to the process at time 0.7 s as explained in the PI discussion. This controller has the ability to keep the shock downstream of the setpoint as the splitter closes. This simulation only temporarily had the shock move upstream of the setpoint and, as desired, no unstart occurred. Notice that with the mixed sensitivity controller there is some overshoot when recovering from the disturbance

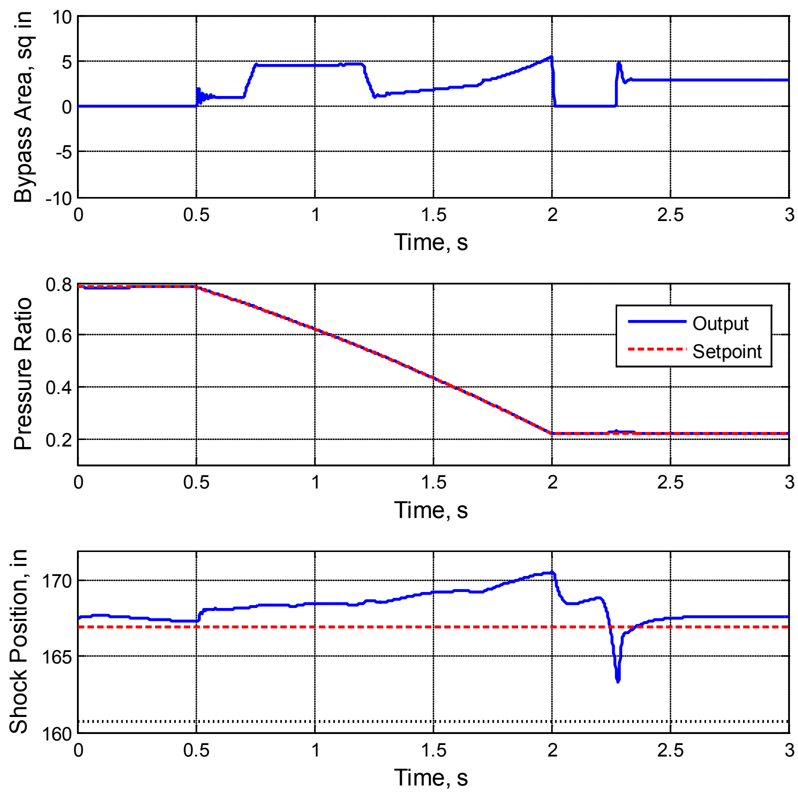

Figure 13.—Control input (top), and shock location (bottom) for the mixed synthesis (H-Infinity) controlled mode transition with a disturbance step added to the system at t = 0.7 s.

Active Disturbance Rejection Control

The active disturbance rejection control has been implemented as discussed in the Shock Position Control Design section. With the plant gain and tuning parameters of b_0 = 1659, ω_c = 502.6548 rad/s, and ω_o = 3141.6 rad/s, the system response with an ADRC controlled mode transition is shown in Figure 14. This is the only controller that does not allow the shock position to move forward of the shock position setpoint during the entire simulation, and does not place the shock aft of 169 in. This controller performs the best in terms of disturbance rejection, disturbance affects shock position the least, and it also has the smallest error between the desired shock position and actual shock location. The ADRC command does have a high frequency control effort which is revealed in the door area plot of Figure 14.

Transient Stability Index Results

The transient stability index created for the scheduled mode transition system, with the open loop method (No), the PI controlled, H-Infinity mixed synthesis (MS) controlled, and ADRC systems at the desired pressure ratio of 0.784 is shown in Figure 15. For a given method, all stability indexes below the line will not unstart the inlet. In addition, any *SI* value below the lowest SI value shown on the plot will not unstart the inlet for any frequency between 1 and 80 Hz. Figure 15 shows a clear advantage in increased operability with the addition of a closed loop control system, while there are only small differences comparing the effectiveness of each closed loop controller. This plot indicates that the system is capable of avoiding inlet unstarts for much larger magnitude disturbances than the open loop controlled method.

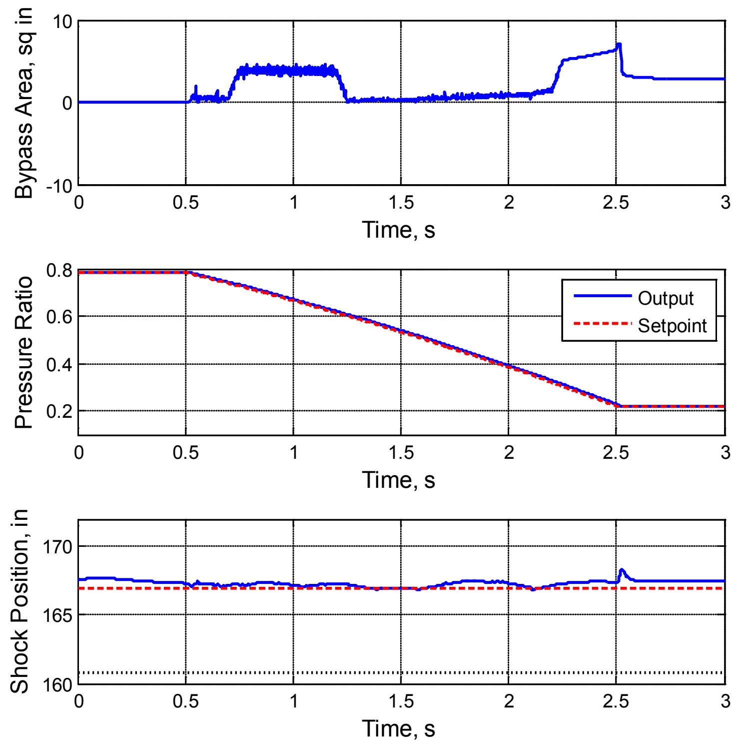

Figure 14.—The control input(top), pressure ratio(middle), and shock location(bottom) for a mode transition with the Active Disturbance Rejection Controller and a disturbance step added to the system.

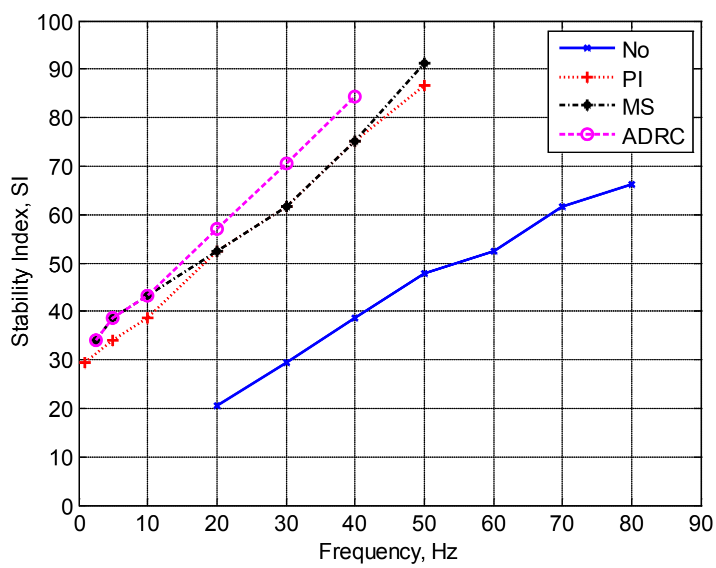

Figure 15.—Transient Stability Index for the scheduled mode transition with the open loop method (No) with a proportional-integral (PI) controller, with a Mixed-Synthesis (MS) controller and with an active disturbance rejection control (ADRC).

Summary and Conclusions

This paper discussed the simulated design and testing of controllers to increase the stability and disturbance rejection capability for a closed-loop mode transition in the Combined Cycle Engine Large-scale Inlet for Mode transition eXperiments (CCE-LIMX). A turbine based combined cycle (TBCC) simulation, known as the High Mach Transient Engine Cycle Code (HiTECC), has been redesigned to replicate the CCE-LIMX. The new simulation replaces the full TBCC propulsion system which included a turbine model, with one which simulated cold pipes and mass flow plugs in place of the turbine, as done with the CCE-LIMX. In order to simulate mode transition, the relationship between the shock position location and pressure ratio at varying splitter angles is determined to create a mode transition schedule, which is also used as the setpoint for the closed loop control system. An open loop control method was used in the mode transition simulation where a bypass door, a control actuator intended to decrease the diffuser exit pressure, was opened as a function of the splitter location. However, when a disturbance was added to this simulation, the inlet unstarted. Three closed loop controllers were designed to reject the disturbances and improve the operability of the inlet. A proportional-integral controller, an H-Infinity mixed synthesis controller, and an active disturbance rejection controller were added to the mode transition simulation. These closed loop controllers were shown to reject the disturbances and avoid unstart. A transient stability index (TSI) plot was created to further compare these closed loop control methods. The transient stability index plot shows the frequency and percent of total airflow (disturbance) that when diverted from a bypass door to the cold pipe resulted in inlet unstart. The closed loop control systems were shown to provide significantly better performance than the inlet without control. In terms of smallest error and disturbance rejection, the best performance was obtained by using the active disturbance rejection controller, which was also shown to have the highest bandwidth and gain. The proportional-integral controller has slightly larger error but a much smoother control signal.

References

1. Sanders, B.W., and Weir, L.J., Aerodynamic Design of a Dual-Flow Mach 7 Hypersonic Inlet System for a Turbine-Based Combined-Cycle Hypersonic Propulsion System, NASA/CR— 2008-215215 (June 2008).
2. Neiner, G.H., Crosby, M.J., Cole, G.L., Experimental and Analytical Investigation of Fast Normal Shock Position Controls for a Mach 2.5 Mixed-Compression Inlet, NASA TN D–6382(July 1971).
3. Cole, G.L., Neiner, G.H., Crosby, M.J., Design and Performance of A Digital Electronic Normal Shock Position Sensor for Mixed-Compression Inlets, NASA TN D–5606 (December 1969).
4. Baumbick, R.J., Neiner, G.H., Cole, G.L., Experimental Dynamic Response of a Two-Dimensional, Mach 2.7 Mixed-Compression Inlet, NASA TN D-6957 (September 1972).
5. Haid, D.A., and Gamble, E.J., Integrated Turbine-Based Combined Cycle Dynamic Simulation Model, 58th Joint Army-Navy-NASA-Air-Force (JANNAF) Interagency Propulsion, Arlington, VA (April 18-22, 2011).
6. Gamble, E.J., Haid, D., D’Alessandro, S., and DeFrancesco, R., Dual-Mode Scramjet Performance Model for TBCC Simulation, AIAA–2009–5298 (August 2009).
7. Gamble, E.J. and Haid, D., Thermal Management and Fuel System Model for TBCC Dynamic Simulation, AIAA 2010-6642, 46th AIAA/ASME/SAE/ASEE Joint Propulsion Conference and Exhibit, Nashville, TN (July 25-28, 2010).
8. Gamble, E.J. and Haid, D., Hydraulic and Kinematic System Model for TBCC Dynamic Simulation, AIAA 2010-6641, 46th AIAA/ASME/SAE/ASEE Joint Propulsion Conference and Exhibit, Nashville, TN, July 25–28, 2010.
9. Csank, J.T., and Stueber, T.J., A Turbine Based Combined Cycle Engine Inlet Model and Mode Transition Simulation Based on HiTECC Tool, AIAA 2012-4149, 48th AIAA/ASME/SAE/ASEE Join Propulsion Conference and Exhibit, Atlanta, GA (July 31–August 1, 2012).

10. Slater, J., Design and Analysis Tool for External-Compression Supersonic Inlets, AIAA-2012-16, Nashville, TN (January 2012).
11. Åström, K. and Hägglund T., PID Controllers: Theory, Design, and Tuning, 2nd Edition, Instrument Society of America, Research Triangle Park, NC (1995).
12. Gao, Z., Active Disturbance Rejection Control: a Paradigm Shift in Feedback Control System Design, American Control Conference, Minneapolis, Minnesota (June 14–16, 2006).
13. Gao, Z., Huang, Y., and Han, J., An Alternative Paradigm for Control System Design, IEEE Conference on Decision and Control (2001).
14. Gao, Z., Scaling and Bandwidth-Parameterization Based Controller Tuning, American Control Conference, Denver, CO (June 2003).
15. Sanders, B.W. and Mitchel, G.A., Throat-Bypass Bleed Systems for Increasing the Stable Airflow Range of a Mach 2.5 Axisymmetric Inlet with 40-Percent Internal Contraction, NASA TM–X–2779 (May 1973).

REPORT DOCUMENTATION PAGE				*Form Approved* *OMB No. 0704-0188*

1. REPORT DATE *(DD-MM-YYYY)*
01-01-2013

2. REPORT TYPE
Technical Memorandum

3. DATES COVERED *(From - To)*

4. TITLE AND SUBTITLE
Shock Position Control for Mode Transition in a Turbine Based Combined Cycle Engine Inlet Model

5a. CONTRACT NUMBER

5b. GRANT NUMBER

5c. PROGRAM ELEMENT NUMBER

6. AUTHOR(S)
Csank, Jeffrey, T.; Stueber, Thomas, J.

5d. PROJECT NUMBER

5e. TASK NUMBER

5f. WORK UNIT NUMBER
WBS 599489.02.07.03.07.11.01

7. PERFORMING ORGANIZATION NAME(S) AND ADDRESS(ES)
National Aeronautics and Space Administration
John H. Glenn Research Center at Lewis Field
Cleveland, Ohio 44135-3191

8. PERFORMING ORGANIZATION REPORT NUMBER
E-18574

9. SPONSORING/MONITORING AGENCY NAME(S) AND ADDRESS(ES)
National Aeronautics and Space Administration
Washington, DC 20546-0001

10. SPONSORING/MONITOR'S ACRONYM(S)
NASA

11. SPONSORING/MONITORING REPORT NUMBER
NASA/TM-2013-217824

12. DISTRIBUTION/AVAILABILITY STATEMENT
Unclassified-Unlimited
Subject Categories: 07 and 63
Available electronically at http://www.sti.nasa.gov
This publication is available from the NASA Center for AeroSpace Information, 443-757-5802

13. SUPPLEMENTARY NOTES

14. ABSTRACT
A dual flow-path inlet for a turbine based combined cycle (TBCC) propulsion system is to be tested in order to evaluate methodologies for performing a controlled inlet mode transition. Prior to experimental testing, simulation models are used to test, debug, and validate potential control algorithms which are designed to maintain shock position during inlet disturbances. One simulation package being used for testing is the High Mach Transient Engine Cycle Code simulation, known as HiTECC. This paper discusses the development of a mode transition schedule for the HiTECC simulation that is analogous to the development of inlet performance maps. Inlet performance maps, derived through experimental means, describe the performance and operability of the inlet as the splitter closes, switching power production from the turbine engine to the Dual Mode Scram Jet. With knowledge of the operability and performance tradeoffs, a closed loop system can be designed to optimize the performance of the inlet. This paper demonstrates the design of the closed loop control system and benefit with the implementation of a Proportional-Integral controller, an H-Infinity based controller, and a disturbance observer based controller; all of which avoid inlet unstart during a mode transition with a simulated disturbance that would lead to inlet unstart without closed loop control.

15. SUBJECT TERMS
Propulsion control; Shock wave control; Feedback control

16. SECURITY CLASSIFICATION OF:			**17. LIMITATION OF ABSTRACT**	**18. NUMBER OF PAGES**	**19a. NAME OF RESPONSIBLE PERSON**
a. REPORT	**b. ABSTRACT**	**c. THIS PAGE**			STI Help Desk (email:help@sti.nasa.gov)
U	U	U	UU	24	**19b. TELEPHONE NUMBER** *(include area code)* 443-757-5802

Standard Form 298 (Rev. 8-98)
Prescribed by ANSI Std. Z39-18